A Novel Approach for Content-based Image Retrieval System using Logical AND and OR Operations

Ranjana Battur[1], Jagadisha Narayana[2]
Dept. of Computer Science and Engineering-Karnataka Law Society's Gogte Institute of Technology, Visvesvaraya Technological University, Belagavi, India[1]
Dept. of Information Science and Engineering, Canara Engineering College, Mangalore Karnataka, India[2]

***Abstract*—This paper proposes an innovative ensemble learning framework for classifying medical images using Support Vector Machine (SVM) and Fuzzy Logic classifiers. The proposed approach utilizes logical AND and OR operations to combine the predictions from the two classifiers, aiming to capitalize on the strengths of each. The SVM and Fuzzy Logic classifiers were independently trained on a comprehensive database of medical images comprising various types of X-ray images. The logical OR operation was then used to create an ensemble classifier that outputs a positive classification if either of the individual classifiers does so. On the other hand, the logical AND operation was used to construct an ensemble classifier that outputs a positive classification only if both individual classifiers do so. The proposed method aims to increase sensitivity and precision by capturing as many positive instances as possible, thereby reducing false positives. The scope of the proposed work is validated in terms of overall time complexity and retrieval accuracy. The simulation outcome shows promising result with 98.36 accuracy score and 1.8 seconds to retrieve all the images in query database.**

***Keywords*—Medical images; support vector machine; fuzzy logic; X-ray images; time complexity**

I. INTRODUCTION

The digital age has led to an explosion of visual content, from personal photos to professional databases. This has created a challenge for users who want to find specific images based on their content. Content-based image retrieval (CBIR) systems are a valuable tool for addressing this challenge [1]. CBIR systems work by extracting visual features from images, such as color, texture, and shape. These features are then used to compare images and find the best matches [2]. This is in contrast to traditional methods of image retrieval, which rely on textual metadata such as tags and keywords. CBIR is especially useful in domains where manual tagging is impractical or where the sheer volume of images makes keyword-based searching insufficient [3]. For example, CBIR can be used to find images of medical conditions, products, or people, even if they are not tagged with the relevant keywords [4]. The uses of CBIR are manifold. For example, in medical imaging, CBIR can help diagnose disease by comparing patient scans to an annotated image database [5]. In the domain of digital libraries, museums, and archival systems, CBIR facilitates the classification, indexing, and retrieval of visual content. Furthermore, e-commerce platforms have the potential to enable customers to search for products using images [6]. The urgency of efficient CBIR systems stems from our increasing reliance on digital visuals [7]. As the volume of digital images continues to grow, the need for intelligent, content-based systems becomes even greater. They not only make the retrieval process more efficient but also open up avenues for more nuanced, context-aware searches, which are often lacking in traditional methods [8].

Despite its potential, CBIR systems face several challenges. One of the biggest challenges is the semantic gap. This is the difference between the low-level visual features extracted by CBIR systems and the high-level semantics understood by users [9-10]. For example, a CBIR system might consider two images to be identical based on their visual features, even if they contain different objects or are taken in different conditions. This can lead to mismatches during retrieval, where the system returns images that are not relevant to the user's query. Another challenge for CBIR systems is the heterogeneity of images. This refers to the fact that images can vary in terms of their angle, scale, lighting conditions, and other factors. This can make it difficult for CBIR systems to accurately match images, even if they contain the same objects [11]. Additionally, images often contain multiple objects, and it can be difficult for CBIR systems to identify the subject of interest [12]. This is especially true for images that are cluttered or have a lot of background noise.

However, even with these advances, there are still challenges to overcome. One challenge is ensuring that CBIR systems are both accurate and time-efficient. This is especially important in specialized domains such as medical imaging, where speed is often critical. Additionally, there is still a gap between machine-extracted features and human interpretation. This can lead to mismatches during retrieval, where the system returns images that are not relevant to the user's query. One possible solution to these challenges is to use an efficient set of classifiers. Our work aims to solve the challenges of CBIR in medical imaging by using an innovative combination of SVM and fuzzy logic. The study believes that this approach can bridge the semantic gap and improve the accuracy and efficiency of CBIR systems in this domain.

This paper introduces a novel approach to CBIR by amalgamating SVM and Fuzzy Logic, harnessing their combined strengths for enhanced image retrieval in the medical domain. The ensemble method, pivoting on logical operations, promises to address the challenges outlined above. The following are the key contributions:

- This paper presents a novel approach to CBIR integrating SVM and fuzzy logic.
- The proposed method aims to bridge the semantic gap that exists between the user's low-level visual features and high-level semantic understanding.
- This article introduces logical AND and OR operations as integration methods within a system. This allows switching between sensitivity and precision based on specific requirements, providing flexibility and adaptability for image retrieval tasks.
- Conduct in-depth analysis of time complexity to set benchmarks for real-time image capture. This contribution is significant, especially in critical areas such as medical imaging where time efficiency is critical.

Following this introduction, the remainder of this paper is organized in a structured manner as follows: Section II offers a brief survey of the existing work, presenting an overview of various methodologies and technologies currently in practice; In Section III, architectural design of the proposed system is discussed along with elucidating the processes of feature database creation, query image formulation, feature extraction, and the intricacies of the retrieval system; Section IV, discusses the system implementation, shedding light on the integration of SVM and Fuzzy Logic in CBIR, and the amalgamation of Ensemble SVM and Fuzzy System using Logical Operations; Section V, present a comprehensive evaluation of our system against a medical imaging database, highlighting the improved precision and recall rates. Finally, Section VI concludes the paper, summarizing the key findings, contributions, and implications of our work. It also outlines the potential avenues for future research, discussing the scalability, adaptability, and possible enhancements to our CBIR system.

II. Related Work

CBIR became known in the early 1990s and gained a lot of attention in research. Over the past decades, different feature extraction techniques have been employed based on appearances such as color, boundary contour, texture, and spatial layout. The work carried out by Younus et al. [13] devised a CBIR system considering color and texture-based feature descriptors and employed a joint approach of k-means and particle swarm optimization (PSO) for image retrieval. The presented scheme is validated on the WANG dataset. Based on the experimental outcome, it is identified that the precision for most classes is improved, but overlooked shape in similarity computations. The study conducted by Sajjad et al. [14] introduced a CBIR system customized to remain invariant to alterations in texture rotation and color features. For color feature extraction, they opted for the HSV color space, and a color histogram was employed for quantization. Notably, to circumvent the effects of illumination changes, only the Hue and Saturation channels were considered. To address rotation variance in textures, they utilized Local Binary Patterns (LBP). The effectiveness of the presented approach is justified based on three datasets namely, Zurich Building, Corel 1 K, and Corel 10 K.

Ashraf et al. [15], combined texture and color in a CBIR approach using HSV color moments, DWT, and Gabor wavelet. Their 1x250 dimensional feature vector improved accuracy but at the cost of slowed searches. The validation of the presented method is done against Corel and GHIM-10 K datasets. Based on the overall outcome analysis it has been identified that the presented method has achieved high precision, but also missing some texture and spatial details. The work presented by Alsmadi et al. [16] addresses the limitations of current CBIR systems by presenting a different scheme that extracts and stores comprehensive color, shape, and texture features as vectors. Techniques include RGB color paired with neutrosophic clustering, YCbCr color with wavelet transform, and gray-level matrices for texture. Utilizing a metaheuristic algorithm for similarity evaluation, the presented model demonstrated superior precision and recall against existing systems. The work of Choe et al. [17] presented an approach leveraging deep learning to retrieve similar chest CT images, aiming to assist examiners in the ILD (interstitial lung disease) diagnosis.

The work carried out by Garg and Dhiman [18] introduces a content-based image retrieval technique that combines discrete wavelet transformation with a rotationally invariant texture descriptor, enhancing feature extraction and reduction. By leveraging magnitude data and GLCM for texture classification, the approach, when tested on the CORAL dataset, demonstrated superior performance across classifiers like SVM, KNN, and decision trees in accuracy and other metrics. It has been observed that the existing CBIR methods falter in multi-class searches due to semantic similarities across image classes. Addressing this, the work of Khan et al. [19] introduces a hybrid CBIR method combining feature descriptors, a genetic algorithm, and an SVM classifier. By integrating color moments, various wavelets, and the L2 Norm for similarity measurement, the method effectively handles class imbalances. Tested on four datasets, it surpassed 25 CBIR techniques in retrieval performance. The authors in the study of Ma et al. [20] introduced a Privacy-preserving CBIR method for cloud-based multimedia, addressing current shortcomings in data encryption and feature extraction. Hybrid encryption is proposed alongside an enhanced DenseNet model for feature extraction from encrypted images. This ensures secure CBIR execution on cloud servers. Tested on two benchmarks, the method outperforms existing solutions by 1.9% and 10% in terms of accuracy, while also reducing computational costs and model parameters significantly.

Monowar et al. [21] introduced, a self-supervised image retrieval system using neural networks (NN), addressing the challenges of expensive or unfeasible data labeling. Trained on pairwise constraints, the model can function in self-supervised environments and with partially labeled datasets. It uses NN to extract and fuse image embeddings for retrieval. Banu et al. [22] explored CBIR using colour and texture features combined with high-level semantics. The proposed system outperforms traditional CBIR systems in speed and efficiency through an ontology model for content analysis when tested on a vast image database. The work of Rani in [23] presented a satellite image retrieval system for forest fire detection using hybrid feature extraction and a unique optimization algorithm

for feature selection; the method shows enhanced precision and recall, surpassing existing fire detection techniques.

Wang et al. [24] introduce a CBIR framework for skin diseases using multi-sourced information. This system fuses dermoscopic, clinical images, and meta-data, and with a graph-based community analysis, boasts a 0.836 precision on the EDRA and ISIC 2019 datasets. Arya and Vimina [25] presented the Local Neighborhood Gradient Pattern (LNGP) for CBIR, capturing local patterns in an 8-bit format. Tests on diverse datasets yield precision ranging from 40.66% to 86.12%, underlining its CBIR efficiency. Madhu and Kumar [26] unveil a hybrid algorithm for medical image feature extraction, merging techniques like DWT, PCA, and GLCM. Using various images, the approach is validated through K-means clustering, with an emphasis on enhancing classification precision via edge detection.

III. Proposed System

This section presents the proposed CBIR system and discusses the implementation procedure adopted to retrieve similar images from the image database. The prime aim of the research work reported in this paper is to evolve with an optimal approach of CBIR while achieving optimal decisions regarding content retrieval with higher precision and retrieval accuracy. In this regard, the study presents a unique and different approach from the existing work where the proposed study locally employs two different models to exploit their decision capability to get optimal results. The schematic depiction of the proposed CBIR system is shown in Fig. 1.

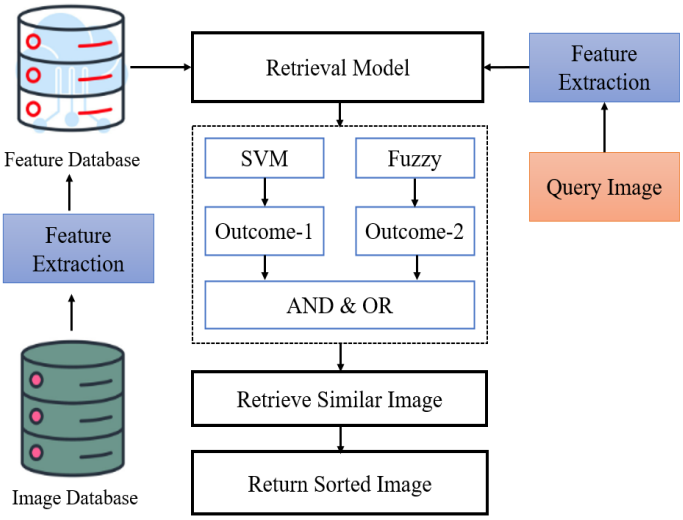

Fig. 1. Schematic architecture of the proposed CBIR system.

As shown in the above Fig. 1, the entire modeling of the proposed system can be divided into three core modules: i) construction of the feature database, ii) query image and its feature extraction, and iii) retrieval system itself. Each of these modules plays a pivotal role in ensuring the efficiency and efficacy of the entire process. Each of these modules plays a pivotal role in ensuring the efficiency and efficacy of the entire process. The system introduced in this paper emphasizes the need to optimize content retrieval, guaranteeing superior precision and accuracy.

A. Construction of Feature Database

This initial module plays a pivotal role in our CBIR approach. It involves meticulously processing the image database to extract and essential features. These features, which serve as unique identifiers for each image, form the foundation of our subsequent retrieval procedures. The system creates a feature-rich database that enables effective comparison and matching by capturing intrinsic characteristics like texture, colour, and shape. The database construction phase is twofold, customized to the distinct feature sets extracted for the SVM and Fuzzy Logic-based systems. For the SVM-based system, the feature extraction process revolves around three pivotal aspects:

- CLD Coefficients: Extracted to capture the spatial distribution of color in images, CLD coefficients provide insights into color layout variations. This feature is integral for distinguishing diverse medical image content.
- Block Division: By dividing images into smaller regions, block division enables localized analysis. This feature facilitates the identification of unique patterns and textures within specific image regions.
- Edge Histogram: Capturing the distribution of edges or gradients within images, the edge histogram feature highlights significant structural information. This attribute contributes to classifying images based on prominent edge distributions.

For the Fuzzy Logic-based system, the feature extraction process encompasses different elements:

- Layer Segmentation: The segmentation of images into distinct layers aids in identifying intricate structures within the medical images. These layers serve as crucial reference points for subsequent comparisons.
- Region of Interest (ROI): Extraction of ROIs isolates specific areas of medical interest. This feature guides the system towards recognizing critical regions with relevance to diagnosis.
- Harris Corner and Fuzzy Corners: Corner detection methodologies like Harris Corner and fuzzy corners enable the identification of distinct points in the image. These points, often representing unique features, enrich the feature database.

B. Query Image and Feature Extraction

The second module addresses the central challenge of CBIR—processing user queries effectively. Each query image presents a unique challenge and opportunity. This module employs advanced techniques to extract pertinent features from the query image. These extracted features are then organized into a structured representation that is well-suited for comparison with the features in our database.

C. Retrieval System

The third module is the heart of our CBIR system. Drawing on the extracted features and processed data from the previous

steps, this module executes the retrieval process. During the retrieval phase, the feature extraction process is applied to the query image. Subsequently, the SVM and Fuzzy Logic models independently process the query image, generating classification outputs based on their respective feature databases. In a harmonious ensemble, the outputs of both SVM and Fuzzy Logic classifiers are combined to derive the final retrieval decision. This amalgamation leverages the unique strengths of both models, enhancing the overall accuracy and robustness of the CBIR system. The diversity of features extracted from the two distinct databases ensures a comprehensive understanding of image content, enabling the system to provide more informed and precise retrieval outcomes.

IV. System Implementation

This section discusses the implementation procedure adopted in the proposed system development.

A. SVM based CBIR

The SVM classifier used in our system is designed for CBIR which operates by extracting significant features from the images, specifically focusing on edge histogram, block division, and color layout descriptor (CLD) features. Block division allows the classifier to consider smaller regions of the image independently, providing local information that can further enhance the classification. CLD encapsulates the spatial distribution of color in the image, another crucial factor in differentiating between various images. It is one of the descriptors defined in the MPEG-7 standard, which is aimed at representing the spatial distribution of color in an image in a very compact form. CLD is highly effective for representing the spatial distribution of colors, even though the descriptor has a very small size. The implementation steps involved in the computation of CLD features are described as follows:

The algorithm begins by reading the input image, which is the target for color distribution analysis. To better represent color information, the image is converted from its original color space to YCbCr. This color space separation allows for a more effective analysis of color distribution. Further, the image is divided into non-overlapping blocks of size 8x8 pixels. If the image's dimensions are not evenly divisible by 8, padding is applied to ensure compatibility. Each block will be processed independently to capture color distribution characteristics. For every 8x8 block, the algorithm calculates the average color value. This is done in the YCbCr color space, where each pixel within the block contributes to the average.

Algorithm-1: CLD Feature Computation

Start:

1. Divide the image into non-overlapping 8x8 blocks
2. Get dimensions (h, w)
3. Blocks: $N_{blocks} = \left\lfloor \frac{h}{8} \right\rfloor \times \left\lfloor \frac{w}{8} \right\rfloor$
4. If $h \,\%\, 8 \neq 0$ or $w \,\%\, 8 \neq 0$
5. do padding to get compatibility with the block size
6. $\forall$ block $B = 1{:}n$
7. compute the average color value
8. $B_{i,j}{:}C_{avg}^{i,j} = \frac{1}{8\times 8} \sum_{y=0}^{7} \sum_{x=0}^{7} B_{i,j}(x,y)$
9. Apply 2D DCT to the 8x8 average color image
10. DCT coefficient for block $B_{i,j}{:}D_{coeff}^{i,j}(u,v) =$
$$\alpha(u)\alpha(v) \sum_{y=0}^{7} \sum_{x=0}^{7} C_{\text{avg}}^{i,j}(x,y) \cos\left(\frac{(2x+1)u\pi}{16}\right) \cos\left(\frac{(2y+1)v\pi}{16}\right)$$
11. The quantized coefficient for block
$$B_{i,j}{:}Q_{\text{coeff}}^{i,j}(u,v) = \text{round}\left(\frac{D_{\text{coeff}}^{i,j}(u,v)}{Q_{\text{table}}(u,v)}\right)$$
12. Arrange quantized DCT coefficients in 1D using zigzag scanning.
$$Z = [Q_{\text{coeff}}^{0,0}, Q_{\text{coeff}}^{0,1}, \ldots, Q_{\text{coeff}}^{7,7}]$$

End

The computed average color values will represent the color essence of each block. The 2D DCT is employed on the average color values of each block. This mathematical transformation converts the spatial color information into frequency components, essential for capturing color distribution patterns. To reduce the amount of data while retaining crucial information, the DCT coefficients are quantized. Quantization involves dividing the coefficients by predefined quantization tables, which effectively reduces their precision. The quantized DCT coefficients are rearranged into a 1D array through zigzag scanning. This process converts the 2D array of coefficients into a compact, linear form, which is crucial for efficient storage and transmission of the descriptor. The resulting 1D array of zigzag-scanned quantized DCT coefficients forms the Color Layout Descriptor (CLD). This descriptor represents the image's color distribution in a highly compact yet informative manner. The computed CLD coefficients can now be used for various applications, such as image retrieval, content analysis, or classification, where the color distribution plays a pivotal role. The second feature namely edge histogram captures the local edge distribution in the image, which has proven to be a significant feature in distinguishing different types of medical images. The implementation steps involved in the computation of edge histogram features are subjected to multiple computing operations. The algorithm first loads the input image, which is then processed for edge histogram computation. To facilitate the process of edge detection, the algorithm transforms the image into grayscale via a weighted combination of its original color channels. This operation yields a single-channel representation where pixel values correspond to intensity levels. To identify edges within the grayscale image, an edge detection algorithm is engaged. This step may encompass techniques such as employing the Sobel or Canny algorithms, adept at highlighting zones of swift intensity fluctuations, often indicative of edges.

The outcome manifests as an edge map, delineating potential edge locations throughout the image. This edge map is then partitioned into discrete, non-overlapping blocks of a predefined magnitude, like 8x8 pixels. The division into smaller blocks fosters simplified analysis and a contextually confined comprehension of edge distribution within the image. For each of these blocks, the algorithm calculates an edge histogram, which quantifies the dispersion of edge orientations within the respective block. This procedure encompasses evaluating the intensity of each pixel's edge and allocating it into predefined bins associated with distinct edge orientations. The individual edge histograms derived from each block are

eventually amalgamated into a singular histogram, encompassing the collective distribution of edge orientations spanning the entire image. This unified histogram forms a succinct representation of how the edges are positioned within the image. The resulting composite histogram, the edge histogram, becomes a versatile asset applicable in diverse contexts. It effectively encapsulates the prevailing edge orientations present in the image and can be harnessed for tasks like image retrieval, object detection, or other undertakings that draw value from insights into the distribution patterns of edges.

Algorithm-2: Edge Histogram Computation

Start:

1. Convert the image to grayscale using a suitable color conversion formula
2. Grayscale intensity at pixel (x, y)
3. $I(x,y) = 0.29 \times R(x,y) + 0.58 \times G(x,y) + 0.11 \times B(x,y)$
4. Apply an edge detection algorithm (e.g., Sobel, Canny) to the grayscale image.
5. $E(x,y)$ represents the edge map resulting from the algorithm
6. Divide the edge map into non-overlapping 8x8 blocks
7. Blocks: $N_{blocks} = \left\lfloor \frac{h}{8} \right\rfloor \times \left\lfloor \frac{w}{8} \right\rfloor$
8. Edge histogram
$$H_{\text{edge}}^{i,j}(k): H_{\text{edge}}^{i,j}(k) = \sum_{y=0}^{7} \sum_{x=0}^{7} \delta(E_{i,j}(x,y), k)$$
9. Combine edge histograms of all blocks into a single
$$H_{\text{combined}}(k): H_{\text{combined}}(k) = \sum_{i=0}^{N_{\text{blocks}}} \sum_{j=0}^{N_{\text{blocks}}} H_{\text{edge}}^{i,j}(k)$$

End

Once the features are extracted, they are organized into a feature vector for each image. This vector becomes the input for the SVM that captures the image's unique characteristics. The extracted features are organized into a feature vector for each image. For example, consider there is m different features extracted for an image, then feature vector can be represented as follows:

$$x = x_1, x_2, x_3 \cdots x_n \tag{1}$$

The combination of the extracted features into a single vector allows the SVM to effectively analyze the image data and make predictions based on these features. The SVM requires training to learn how to distinguish between different classes or categories. SVM learns to find a hyperplane that maximizes the margin between classes. The optimization problem involves finding the optimal $\overline{w}$ and $\overline{b}$ that define the hyperplane while considering misclassified points. SVM is a supervised learning model used for classification and regression tasks. The fundamental idea behind SVM is to find a hyperplane that best separates data points of different classes while maximizing the margin between these classes. This hyperplane serves as the decision boundary for classification, and the data points closest to the hyperplane are known as support vectors. Given a set of training data $X = (x_1, y_1), (x_2, y_2) \cdots (x_n, y_n)$, where x_i represents the feature vector and y_i is the corresponding class label (either +1 or -1), the SVM aims to find a hyperplane $w \cdot x + b =$, that separates the two classes. The distance between the hyperplane and the support vectors is given by the margin, which is proportional to $1/||w||$. The optimization problem for SVM can be formulated as follows:

$$min: ||w||^2 + C \sum_{i=1}^{n} \xi_i \tag{2}$$

$$\text{subjected to: } y_i(w \cdot x + b) \geq 1 - \xi_i, s.t \xi_i \geq 0$$

where, C denotes a regularization parameter that balances the trade-off between maximizing the margin and minimizing the classification error, and ξ_i slack variables that allow for misclassified points or points within the margin. The goal is to minimize the value of $||w||$, while satisfying the classification constraints.

For image retrieval, a user provides a query image. The same feature extraction and vectorization process is applied to the query image. The SVM requires training to learn how to distinguish between different classes or categories. In the context of image retrieval, each image is assigned a label indicating its category. During training, the SVM constructs a decision boundary, known as a hyperplane that optimally separates the feature vectors of different classes. This hyperplane maximizes the margin between classes, effectively determining the most discriminative features for classification. Once the SVM is trained, it can be used for classification. For image retrieval, a user provides a query image that needs to be classified and compared against the images in the database. The query image undergoes the same feature extraction and vectorization process as the training images. The trained SVM then assesses the query image's feature vector and places it on the appropriate side of the decision boundary, classifying it into one of the predefined categories.

The SVM-based image retrieval process doesn't end with classification. Instead, it ranks the retrieved images based on their proximity to the decision boundary. Images that are closer to the decision boundary are considered more similar to the query image in terms of their feature characteristics. As a result, these images are ranked higher in the retrieval process. Finally, the retrieved images are presented to the user in the order of their ranking. Images that closely match the query image's features are displayed at the top of the list, providing the user with the most relevant results first.

B. Fuzzy System-based CBIR

The Fuzzy Logic-based classifier in our system focuses on edge detection for image retrieval. Edge detection is a fundamental tool in image processing and is critical in segmenting regions of interest in medical images. By employing Fuzzy Logic, the classifier can handle the inherent uncertainty and imprecision in edge detection, leading to a more robust image retrieval. The initial step involves extracting relevant features from the images. This could include processes such as median filtering, ROI extraction, and Harris corner detection. The outcome of this step is a collection of extracted features that serve as inputs to the subsequent fuzzy logic framework. Next, layer segmentation involves partitioning images into discrete layers. This process aids in the identification and isolation of intricate structures within medical images. Mathematically, the layer segmentation can be represented as dividing the image I into n distinct layers such

that: $L_1, L_2, L_3, \cdots L_n$ where n denotes the number of layers; further, extracting Regions of Interest (ROIs) involves isolating specific areas within the images that hold medical relevance. Mathematically, an ROI can be defined as a subset of pixels within an image I defined by a set of coordinates (x, y) that denote the spatial bounds of the ROI. Corner detection techniques like Harris corners and fuzzy corners identify distinct points in the image. These points often correspond to unique features that contribute to the overall understanding of the image. Mathematically, Harris corner detection involves evaluating the corner response function R for each pixel in the image and identifying points with high corner responses. The implementation steps for computing Harris corner and fuzzy corners features are discussed in Algorithm 3.

The algorithm presented is a comprehensive approach for detecting both Harris corners and Fuzzy Corners within grayscale images. Starting with the Harris Corner Detection, the algorithm initially computes the gradients of the image using derivative filters, followed by the calculation of products of gradients and their smoothing through a Gaussian filter. The Harris response function is then computed for each pixel, reflecting the intensity of corner features. Non-maximum suppression is applied to identify potential corner locations, and a threshold is set to retain corners with significant Harris responses. However, what sets this algorithm apart is the incorporation of Fuzzy Corners. For each detected Harris corner, a degree of "cornerness" is calculated using a sigmoidal membership function (step-9). This degree of cornerness adds a layer of nuance to the corner detection, capturing the intensity of corners in a fuzzy manner. Linguistic variables are introduced to categorize corners based on their degree of cornerness, offering a more comprehensive understanding of corner characteristics. By combining traditional corner detection with fuzzy logic, the algorithm enhances the corner detection process. The inclusion of fuzzy degrees of corners brings a new dimension to corner characterization, allowing for a more nuanced representation of corner features within images. This approach is particularly valuable in scenarios where corners exhibit varying degrees of intensity, contributing to a richer understanding of image content. In essence, this algorithm presents a holistic framework for corner detection that embraces both crisp corner points and the fuzzy characterization of corner intensity, broadening the scope of corner analysis in image processing. The image retrieval process based on the provided steps involves a unique approach that combines fuzzy logic with the concepts of similarity measurement and defuzzification.

Algorithm-3: Harris Corner and Fuzzy Corners Detection

Input: Grayscale image I of size $M \times N$, Threshold T for corner intensity

Output: Sets of detected Harris corners and Fuzzy Corners

Start:

1. Convert the image I into gradients I_x and I_y
2. Compute the products of gradients ∀ pixel:
$$I_x^2, I_y^2 \text{ and } I_{xy} = I_x \cdot I_y$$
3. Apply a Gaussian filter to smooth the computed products:
$$S_{I_x^2}, S_{I_y^2} \text{ and } S_{I_{xy}}$$
4. Compute the Harris response function for each pixel
$$R = det(M) - k \times trace(M)^2$$
Where M is the matrix of second-order derivatives, k is an empirical constant (between 0.04 and 0.06),
$$det(M) = S_{I_x^2}, \cdot S_{I_y^2} - S_{I_{xy}} \text{ and}$$
$$trace(M) = S_{I_x^2}, + S_{I_y^2}$$
5. Apply non-maximum suppression to identify potential corner locations.
6. Set a threshold T, on R and retain corners with R above the threshold
7. Process: Fuzzy Corners
8. ∀C
9. compute the degree of corners using a membership function:
$$degreeofcornerness(C) = \frac{1}{1 + e^{-\alpha \cdot R(C)}}$$
Where $R(C)$ is the Harris response at corner C, and α is a tuning parameter that controls the steepness of the membership curve.
10. Define linguistic variables low cornerness, moderate cornerness, and high cornerness using appropriate fuzzy sets.
11. Categorize each detected corner into one of the fuzzy sets based on its degree of corners
12. Return:
Sets of detected Harris corners and their corresponding degrees of corners (fuzzy membership values)
Categorized Fuzzy Corners based on their degree of corners

End

The adopted computing process offers a unique perspective on image similarity, enhancing the traditional methods used for content-based image retrieval. In the image retrieval, the degree of similarity between a query image and a database image is computed using fuzzy logic. This step capitalizes on the capability of fuzzy rule-based systems to handle imprecision and variability in data. Fuzzy rules are defined to establish relationships between the features of the query image and the database image, leading to the determination of similarity. The membership functions used in the proposed algorithm are defined based on the three factors viz. (i) $\mu_Q(Q)$ Is the membership function for the query image's high corner intensity (HCI), (ii) $\mu_D(D)$ is the membership function for the database image's HCI, and iii) $\mu_S(S)$ is the membership function for the degree of Similarity. Here, the variable Q represents the degree of HCI in the query image, similarly variable D represents the degree of HCI in the database image and variable S represents the degree of similarity between the query and database images. Using these variables and membership functions, the fuzzy rules are defined as follows:

$$\text{IF } Q = \text{High AND } D = \text{High, THEN } S = \text{HIGH} \quad (3)$$

$$\text{IF } Q = \text{Low AND } D = \text{Low, THEN } S = \text{Low} \quad (4)$$

These rules allow for a flexible interpretation of image similarity. If both the query image and the database image possess high corner intensities, their similarity is rated as high.

Conversely, if either the query or database image has low corner intensities, the similarity is considered low. However, the algorithm does not consider the logic for MEDIUM as it can lead to introduce redundancy, increase complexity, and may not add substantial value to the ranking and retrieval process. While the concept of a "Medium" category could theoretically represent a middle ground in corner intensities and hence, medium similarity, its practical implementation may not be as meaningful or effective given that the inherent numerical nature of intensities already provides a continuous scale of similarity. Therefore, the presented approach provides a nuanced way of assessing similarity based on multiple factors, leading to more contextually relevant image retrieval.

C. Ensemble SVM and Fuzzy System using Logical Operation

The proposed ensemble learning approach ingeniously integrates the SVM and Fuzzy Logic classifiers by employing logical AND and OR operations. Given an input x, the outputs of the OR operation-based ensemble $Y_{OR}(x)$ and the AND operation-based ensemble $Y_{AND}(x)$ can be expressed as follows:

$$Y_{OR}(x) = SVM(x) \vee Fuzzy(x) \quad (5)$$

$$Y_{AND}(x) = SVM(x) \ \wedge Fuzzy(x) \quad (6)$$

where, *SVM(x)* represents the binary outputs of the SVM classifier and *Fuzzy(x)* refers to Fuzzy Logic classifiers, respectively. The symbols $\vee$ and $\wedge$ represent the logical OR and AND operations, respectively. In this new ensemble learning system, the OR-based ensemble predicts an instance to be positive if either the SVM or the Fuzzy Logic classifier predicts it to be positive. This arrangement increases the system's sensitivity by capturing more positive instances but also slightly increases the risk of false positives. Conversely, the AND-based ensemble predicts an instance to be positive only if both classifiers predict it to be positive. This increases the system's precision by reducing the risk of false positives but also slightly increases the risk of missing some true positives. This ensemble learning system aims to provide a more adaptable and robust solution for the challenging task of medical image classification by strategically leveraging the complementary strengths of both classifiers. In the OR operation, the ensemble essentially combines the outputs of both classifiers using majority voting. If the SVM or Fuzzy Logic classifier predicts a positive class, the ensemble also predicts a positive one. On the other hand, the AND operation involves constructing a meta-model that integrates the predictions of both classifiers. The ensemble only predicts a positive class if the SVM and Fuzzy Logic classifiers agree on the classification outcome. By intelligently fusing their decision-making capabilities through logical operations, the system ensures a more adaptable and resilient solution for the intricate task of medical image classification, addressing the need for sensitivity and precision in different clinical contexts. Algorithm 4 outlines a systematic process for combining SVM and Fuzzy Logic classifiers through ensemble learning. It involves training both classifiers using distinct features and then classifying test instances using both classifiers. The results from SVM and Fuzzy Logic classifiers are combined using logical operations to create two ensemble results. Depending on the outcomes of these ensemble results, instances are classified as positive. This approach allows for harnessing the strengths of both classifiers, contributing to a more robust and flexible image classification system.

Algorithm-4: Ensemble Learning Using AND and OR

Inputs:
$\mathcal{D}_{image}$ (Train Data attributed to Image Database)
$\mathcal{D}_{query}$ (Test Data attributed to Query Database)
Outputs:
$\mathcal{R}_{\mathrm{OR}}$ (results from the OR operation-based ensemble)
$\mathcal{R}_{\mathrm{AND}}$ (results from the AND operation-based ensemble)
Start

1. Initialize Classifiers
   SVM classifiers: $\mathcal{C}_{SVM}$
   Fuzzy logic classifier: $\mathcal{C}_{FL}$
2. Classifier: $\mathcal{C}_{SVM}$
   Extract feature $\mathcal{F}_{SVM}$ including edge histogram, block division, and color layout
   Train $\mathcal{C}_{SVM}$ using $\mathcal{D}_{image}$ and $\mathcal{F}_{SVM}$
3. Classifier: $\mathcal{C}_{FL}$
   Apply Fuzzy Logic-based edge detection on to obtain edge features $\mathcal{F}_{\mathrm{Fuzzy}}$
   Train Classifiers $\mathcal{C}_{FL}$ using $\mathcal{D}_{\mathrm{image}}$ and $\mathcal{F}_{\mathrm{Fuzzy}}$
4. Classify test instances
   For each instance x_i in $\mathcal{D}_{query}$:
   Extract relevant features $\mathcal{F}_i$ from instance
   Obtain SVM classification result:
   $y_{SVM}(x_i) = \mathcal{C}_{SVM}(\mathcal{F}_i)$
   Perform Fuzzy Logic-based edge detection to extract edge features $\mathcal{F}^{\mathrm{i}}_{\mathrm{Fuzzy}}$ from instance
   Obtain Fuzzy Logic classification result:
   $y_{FL}(x_i) = \mathcal{C}_{FL}\ (\mathcal{F}^{\mathrm{i}}_{\mathrm{Fuzzy}})$
5. Ensemble Classifications
   For each instance x_i in $\mathcal{D}_{query}$:
   Compute AND ensemble:
   $y_{AND}(x_i) = y_{SVM}(x_i) \wedge y_{FL}(x_i)$
   Compute OR ensemble:
   $y_{OR}(x_i) = y_{SVM}(x_i) \vee y_{FL}(x_i)$
6. Return
   $\mathcal{R}_{\mathrm{OR}}$ consisting of all $y_{OR}(x_i)$
   $\mathcal{R}_{\mathrm{AND}}$ consisting of all $y_{AND}(x_i)$

End

V. Result Analysis

The proposed CBIR system was designed and developed using the Matlab and Python computing environments. The system was implemented on a Windows 10, core i7, system type 64-bit with 16GB RAM. The performance analysis of the proposed system is primarily carried out concerning retrieval accuracy and processing time with support of extensive discussion.

A. Image Database Adopted

In this study a custom dataset comprising multi-modal images were created to evaluate the proposed CBIR system. The custom dataset was primarily based on the UNIFESP dataset, which contains 2,481 medical images. However, the study did not use all the images from this dataset. Instead, it used 1,500 images from UNIFESP and 858 images from other

sources. The experimental analysis was performed on a custom dataset of 1,920 images, which was divided into a training set (database) of 1,482 images and a test set (query database) of 438 images. The rationale behind this choice lies in the limited availability of comprehensive multi-modality datasets and as intended application of the proposed CBIR system is to facilitate analysis which should imitates real-world scenarios where users frequently search for diverse images. The database comprises a wide range of medical images, encompassing chest, hand, and ankle X-rays.

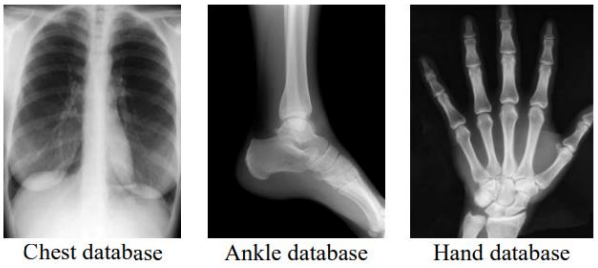

Fig. 2. Sample visualization of images in the database.

As shown in Fig. 2 above, the images are sourced from authoritative medical repositories and are characterized by their clinical relevance. Including medical images caters to the system's applicability in healthcare, enabling accurate retrieval of specific anatomical regions for diagnosis and reference.

B. Visual Analysis of SVM Feature Descriptor

This section presents a visual analysis of the features descriptor obtained for the SVM-based CBIR system. The analysis provided for testing Ankle X-ray images from the query database.

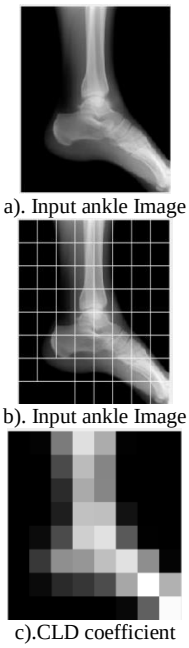

Fig. 3. Visual analysis of feature descriptor for SVM.

Fig. 3(a) shows that the initial image chosen for analysis is an Ankle X-ray image from the dataset. In Fig. 3(b) here, the same input Ankle X-ray image is displayed to provide a precise reference for subsequent feature analyses. In Fig. 3(c), the Color Layout Descriptor (CLD) coefficients is exhibited, illustrating the spatial distribution of colours in the input Ankle X-ray image.

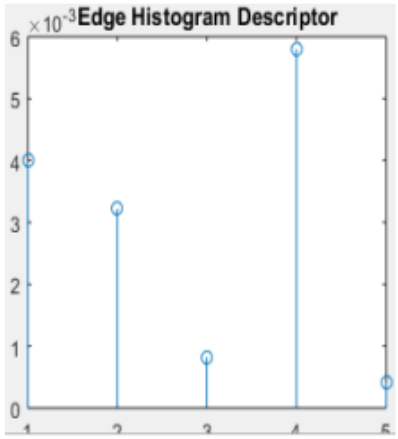

Fig. 4. Edge histogram descriptor

Fig. 4 present the edge histogram descriptor, which encapsulates the distribution of local edges in the image. This descriptor contributes to the system's ability to differentiate various image regions based on edge patterns. This visual analysis succinctly showcases the various feature descriptors generated by the SVM-based CBIR system. These descriptors are instrumental in enabling the system to capture distinct characteristics of the input image, facilitating effective content-based retrieval. This section gives readers insight into the transformative impact of feature extraction on the CBIR process.

C. Visual Analysis of Fuzzy Feature Descriptor

This section presents a visual analysis of the features descriptor obtained for a fuzzy-based CBIR system. The analysis provided for testing Ankle X-ray images from the query database.

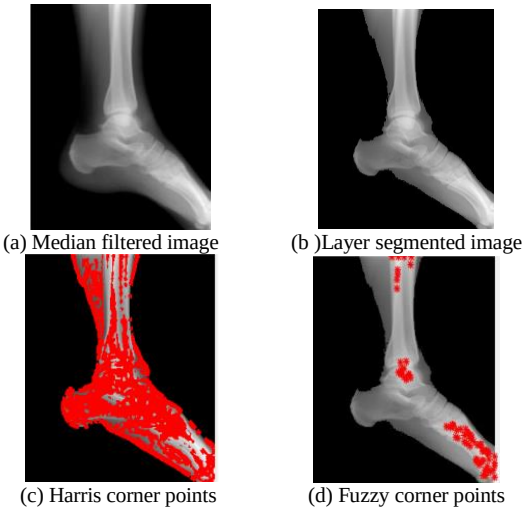

Fig. 5. Visual analysis of fuzzy feature descriptor.

In Fig. 5, a comprehensive visual analysis of the feature descriptors derived from the Fuzzy-based CBIR system, is

meticulously presented. Fig. 5(a) unveils the image after undergoing median filtering. This procedure smoothens the image, reducing noise while retaining essential structural information, rendering it an ideal input for subsequent analyses. Fig. 5(b) showcases the outcome of the layer segmentation process applied to the Ankle X-ray image. This segmentation facilitates the identification of distinct anatomical layers, facilitating precise feature extraction. The image depicted in Fig. 5(c) illustrates the Harris corner points, which are crucial for pinpointing distinctive features within the image. These points serve as significant landmarks in the feature extraction process. Fig. 5(d) brings forth the Fuzzy corner points, representing unique features identified within the image. These points contribute to the descriptor generation process, encapsulating salient attributes for retrieval. This visual analysis provides a profound understanding of the diverse feature descriptors synthesized by the Fuzzy-based CBIR system. These descriptors contribute to capturing intricate characteristics embedded within the input image. By navigating this section, readers better understand how feature extraction through Fuzzy Logic contributes to the CBIR process, enhancing the system's aptitude for content-based image retrieval.

D. Performance Analysis Concerning Retrieval Accuracy

The cornerstone of any CBIR system lies in its ability to retrieve relevant images based on user queries accurately. In the context of our proposed system, retrieval accuracy serves as a critical indicator of success. The assessment measures the proportion of retrieved images genuinely relevant to the query, thus quantifying the system's ability to discern and match image features. A high retrieval accuracy validates the efficacy of our approach in effectively capturing and exploiting distinctive features for content-based retrieval. The retrieval accuracy is calculated as a percentage, reflecting the proportion of correctly retrieved relevant images out of the total number of relevant images. This metric quantitatively assesses the CBIR system's ability to accurately identify and retrieve images that match the user's intent.

$$Retrieval\ Accuracy = \frac{Number\ of\ Relevant\ Images\ Retrieved}{Total\ Number\ of\ Relevant\ Images} \times 100$$

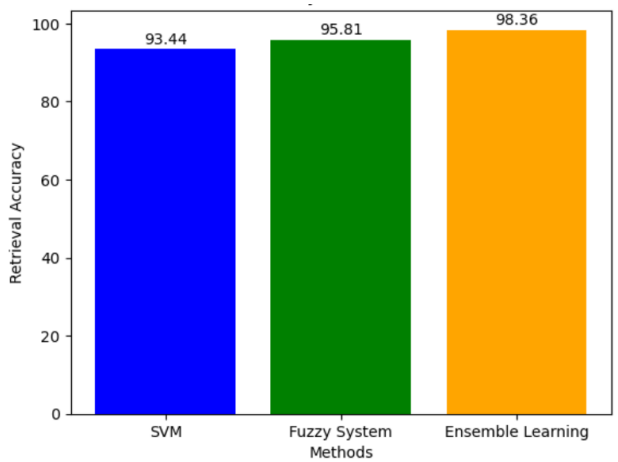

Fig. 6. Analysis of retrieval accuracy.

The results demonstrated in Fig. 6 clearly showcase the performance outcomes of each retrieval model, SVM, Fuzzy System, and Ensemble Learning. The SVM-based CBIR model demonstrates a retrieval accuracy of 93.44%. However, despite its high accuracy, SVM might encounter challenges in handling the intricacies of image data due to its linear nature. This limitation can lead to a slightly lower accuracy when compared to more adaptable models. The Fuzzy-based CBIR model exhibits an impressive retrieval accuracy of 95.35%. This higher accuracy can be attributed to the nature of Fuzzy Logic, which accommodates uncertainty and imprecision in image data. Fuzzy Logic is particularly well-suited for image segmentation and feature extraction, as it can handle varying degrees of membership. The Ensemble Learning-based CBIR model outshines the others with a remarkable retrieval accuracy of 98.36%. This higher accuracy can be attributed to the model's ability to harness the strengths of both SVM and Fuzzy Logic. The ensemble approach intelligently combines the decisions of these models using logical operations, striking a balance between precision and sensitivity. By doing so, it minimizes the weaknesses of individual models and leverages their combined potential. The SVM model provides a strong baseline, while the Fuzzy Logic model's adaptability enhances accuracy. The Ensemble Learning approach capitalizes on the synergies between SVM and Fuzzy Logic, leading to the highest accuracy due to its ability to adapt to different images and decision scenarios.

E. Performance Analysis Concerning Processing Time

While retrieval accuracy is paramount, it must be complemented by efficient processing time. The CBIR system's speed is integral, particularly in real-world scenarios where rapid responses are vital. The proposed system's processing time is evaluated as a measure of its computational efficiency. Lower processing times enhance user experience and render the system suitable for time-critical applications.

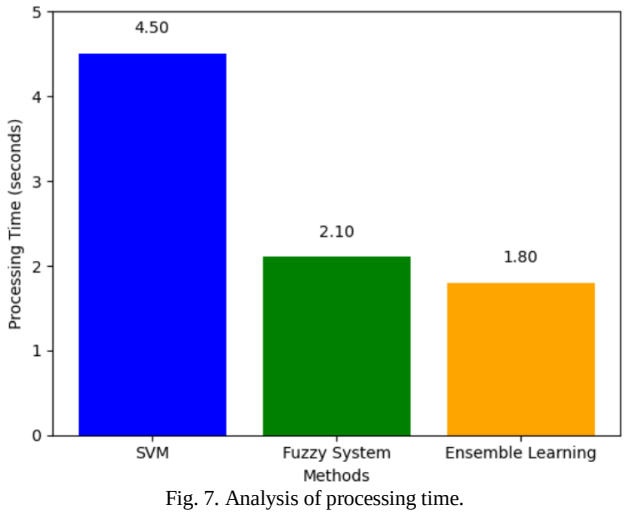

Fig. 7. Analysis of processing time.

The above Fig. 7 presents the performance analysis of the proposed system in terms of system response time for the different CBIR models, namely, SVM-CBIR, Fuzzy-CBIR, and Ensemble-CBIR. SVM-CBIR exhibits a longer processing time of 4.50 seconds on average. This can be due to the inherent complexity of the SVM's training process. Training of

SVMs involves iteratively optimizing the decision boundary that effectively separates the different classes. This process can lead to longer processing times in medical imaging scenarios, where datasets can be extensive and feature spaces complex. Fuzzy-CBIR, in contrast, exhibits a lower average processing time of 2.10 seconds. This efficiency is mapped to the nature of fuzzy logic operations, which handle membership degrees and linguistic variables. These operations enable quick calculations and quick decision-making. The processing efficiency of fuzzy-CBIR makes it particularly suitable for applications where quick retrieval with approximate similarity estimation is sufficient. The Ensemble-CBIR model balances accuracy and efficiency with an average processing time of 1.80 seconds. By combining the strengths of both SVMs and fuzzy logic classifiers through logical operations, the group adapts to the accuracy and sensitivity requirements. Although slightly higher than Fuzzy-CBIR due to Ensemble operation calculations, Ensemble-CBIR is more efficient than SVM-CBIR. This balance makes it an attractive solution for various medical image retrieval scenarios.

It is to be noted that the analysis of system processing time is also directly related to the time complexity analysis, which can be described as follows: The time complexity of the SVM-based CBIR model primarily revolves around two main phases: training and testing. The training phase involves extracting features from the training images and training the SVM model. If we denote the number of training images as 'n' and the number of features as m, the time complexity of feature extraction is typically $O(n \times m)$. The training of the SVM model will be $O(n \times m^2)$. Similar to the training phase, feature extractions and classification have a time complexity of $O(m)$. Several factors influence the time complexity of the Fuzzy Logic-based CBIR model. Edge detection and feature extraction involve processing each pixel of an image. If 'n' represents the number of pixels in an image, the time complexity for these steps is generally $O(n)$. Fuzzy Logic classification evaluates the fuzzy rules for each feature. The number of fuzzy rules and their complexity affect the time complexity, but it's typically $O(1)$ for each feature. The time complexity for testing the Ensemble model depends on the testing time of both SVM and Fuzzy Logic classifiers and the time complexity of the ensemble operation ($ORorAND$). If we denote the time complexities of SVM and Fuzzy Logic testing as T_{svm} and T_{fuzzy}, respectively, and the time complexity of ensemble operation as $T_{ensemble}$, the overall time complexity can be approximated as $O(T_{svm} + T_{fuzzy} + T_{ensemble})$.

Hence, the time complexity analysis highlights that Fuzzy-CBIR generally has a lower time complexity due to its more effective feature extraction process. At the same time, SVM-CBIR and Ensemble-CBIR involve more complex feature extraction and classification steps.

VI. Conclusion

This paper significantly contributes to content-based image retrieval (CBIR) systems. The authors explore a variety of methodologies, including support vector machines (SVMs), fuzzy logic, and ensemble learning, to develop an advanced CBIR system with potential applications beyond medical imaging. The proposed system's retrieval accuracy and processing efficiency have been empirically validated, demonstrating its effectiveness in providing precise results promptly. The adaptable ensemble learning approach, which combines the strengths of established techniques, provides a balanced solution for diverse image retrieval scenarios. While this paper has made significant strides in the development of an effective and lightweight CBIR system, there remain several promising scopes for future research and improvement. In the future, the proposed work will be extended towards automated feature extraction process leveraging potential of the deep learning-based approaches to capture new and latent image characteristics, leading to even more precise retrieval results in dynamic and complex scenarios. In future, the study will evolve to incorporate multi-modal data combining medical images with textual patient records to offer a more comprehensive and context-aware CBIR system, especially in healthcare settings.

References

[1] Latif et al., "Content-Based Image Retrieval and Feature Extraction: A Comprehensive Review," Mathematical Problems in Engineering, vol. 2019, pp. 1–21, Aug. 2019, doi: 10.1155/2019/9658350.

[2] M. N. Abdullah et al., "Colour Features Extraction Techniques and Approaches for Content-Based Image Retrieval (CBIR) System," Journal of Materials Science and Chemical Engineering, vol. 09, no. 07, pp. 29–34, 2021, doi: 10.4236/msce.2021.97003.

[3] Sarath Chandra Yenigalla, S. Rao, and Ngangbam Phalguni Singh, "Implementation of Content-Based Image Retrieval Using Artificial Neural Networks," Engineering Proceedings, Mar. 2023, doi: 10.3390/hmam2-14161.

[4] S. Sikandar, R. Mahum, and A. Alsalman, "A Novel Hybrid Approach for a Content-Based Image Retrieval Using Feature Fusion," Applied Sciences, vol. 13, no. 7, p. 4581, Jan. 2023, doi: 10.3390/app13074581.

[5] S. M. Anwar, M. Majid, A. Qayyum, M. Awais, M. Alnowami, and M. K. Khan, "Medical Image Analysis using Convolutional Neural Networks: A Review," Journal of Medical Systems, vol. 42, no. 11, Oct. 2018, doi: https://doi.org/10.1007/s10916-018-1088-1.

[6] C. B. Akgül, D. L. Rubin, S. Napel, C. F. Beaulieu, H. Greenspan, and B. Acar, "Content-Based Image Retrieval in Radiology: Current Status and Future Directions," Journal of Digital Imaging, vol. 24, no. 2, pp. 208–222, Apr. 2010, doi: 10.1007/s10278-010-9290-9.

[7] C. DeLorenzo, X. Papademetris, L. H. Staib, K. P. Vives, D. D. Spencer, and J. S. Duncan, "Image-Guided Intraoperative Cortical Deformation Recovery Using Game Theory: Application to Neocortical Epilepsy Surgery," IEEE Transactions on Medical Imaging, vol. 29, no. 2, pp. 322–338, Feb. 2010, doi: 10.1109/tmi.2009.2027993.

[8] K. Juneja, A. Verma, S. Goel and S. Goel, "A Survey on Recent Image Indexing and Retrieval Techniques for Low-Level Feature Extraction in CBIR Systems," 2015 IEEE International Conference on Computational Intelligence & Communication Technology, Ghaziabad, India, 2015, pp. 67-72, doi: 10.1109/CICT.2015.92.

[9] B. Ergen and M. Baykara, "Texture based feature extraction methods for content based medical image retrieval systems," Bio-Medical Materials and Engineering, vol. 24, no. 6, pp. 3055–3062, 2014, doi: 10.3233/bme-141127.

[10] N. Borah and Udayan Baruah, "Feature Extraction Techniques for Shape-Based CBIR—A Survey," Springer eBooks, pp. 205–214, Dec. 2021, doi: 10.1007/978-981-16-4244-9_16.

[11] R. Battur and J. N., "CBIR System Development Using the Concepts of Image Feature Synthesis with Matching Parameters-A Survey," Journal of Communication Engineering and its Innovations, vol. 7, no. 1, Apr. 2021, doi: 10.46610/jocei.2021.v07i01.006.

[12] B. Patel, K. Yadav, and D. Ghosh, "Current Trend and Methodologies of Content-Based Image Retrieval: Survey," Algorithms for intelligent systems, pp. 647–665, Jan. 2021, doi: 10.1007/978-981-15-6707-0_64.

[13] Z. S. Younus, D. Mohamad, T. Saba, H. M. Alkawaz, A. Rehman, M. Al-Rodhaan, and A. Al-Dhelaan, "Content-based image retrieval using PSO and k-means clustering algorithm," Arabic Journal Geoscience, vol. 8, no. 8, pp. 6211–6224, 2015.

[14] M. Sajjad, A. Ullah, J. Ahmad, N. Abbas, S. Rho, and S. W. Baik, "Integrating salient colors with rotational invariant texture features for image representation in retrieval systems," Multimedia Tools and Applications, vol. 77, no. 4, pp. 4769–4789, Feb. 2018.

[15] R. Ashraf, M. Ahmed, U. Ahmad, M. A. Habib, S. Jabbar, and K. Naseer, "MDCBIR-MF: Multimedia data for content-based image retrieval by using multiple features," Multimedia Tools and Applications, vol. 79, no. 13–14, pp. 8553–8579, Apr. 2020.

[16] M. K. Alsmadi, "Content-Based Image Retrieval Using Color, Shape and Texture Descriptors and Features," Arab J Sci Eng, vol. 45, pp. 3317–3330, 2020.

[17] J. Choe et al., "Content-based image retrieval by using deep learning for interstitial lung disease diagnosis with chest CT," Radiology, vol. 302, no. 1, pp. 187-197, 2022.

[18] M. Garg and G. Dhiman, "A novel content-based image retrieval approach for classification using GLCM features and texture fused LBP variants," Neural Comput & Applic, vol. 33, pp. 1311–1328, 2021.

[19] U. A. Khan, A. Javed, and R. Ashraf, "An effective hybrid framework for content based image retrieval (CBIR)," Multimed Tools Appl, vol. 80, pp. 26911–26937, 2021.

[20] W. Ma et al., "A privacy-preserving content-based image retrieval method based on deep learning in cloud computing," Expert Systems with Applications, vol. 203, p. 117508, 2022.

[21] M. M. Monowar et al., "AutoRet: A self-supervised spatial recurrent network for content-based image retrieval," Sensors, vol. 22, no. 6, p. 2188, 2022.

[22] J. Faritha Banu et al., "Ontology Based Image Retrieval by Utilizing Model Annotations and Content," in 2022 12th International Conference on Cloud Computing, Data Science & Engineering (Confluence), Noida, India, 2022, pp. 300-305.

[23] K. V. Rani, "Content based image retrieval using hybrid feature extraction and HWBMMBO feature selection method," Multimed Tools Appl, 2023.

[24] Y. Wang et al., "Multi-channel content based image retrieval method for skin diseases using similarity network fusion and deep community analysis," Biomedical Signal Processing and Control, vol. 78, p. 103893, 2022.

[25] R. Arya and E. R. Vimina, "Local neighborhood gradient pattern: A feature descriptor for content based image retrieval," Journal of Intelligent & Fuzzy Systems, vol. 43, no. 4, pp. 4477-4499, 2022.

[26] R. Madhu and Kumar, "A hybrid feature extraction technique for content based medical image retrieval using segmentation and clustering techniques," Multimed Tools Appl, vol. 81, pp. 8871–8904, 2022.